A safety oriented decision support tool for the remanufacturing and recycling of post-use H&EVs Lithium-Ion batteries

Luca Gentilini [a,*], Elena Mossali [b], Alessio Angius [a], Marcello Colledani [a,b]

[a] Department of Mechanical Engineering, Politecnico di Milano, Via la Masa 1, 20156 Milan, Italy
[b] STIIMA-CNR Institute of Intelligent Industrial Technologies and Systems for Advanced Manufacturing, National Research Council, Via Alfonso Corti 12, 20133 Milan, Italy

ARTICLE INFO

ABSTRACT

The battery is a key component of electric vehicles. To reach the needed voltage and capacity, single Lithium-Ion cells are assembled into modules, then assembled into the pack. Their disassembly, which unlocks both remanufacturing or recycling and which nowadays is made mainly manually, has high electric hazards. Decision tools have not yet been developed to minimize these risks. This work presents a mathematical model to determine the disassembly sequence with the minimal exposure of the operator to hazardous voltages. The model considers the mechanical and electrical architecture of the battery and the tasks needed to reach the desired disassembly level.

1. Introduction

The transition from conventional combustion cars to hybrid and full electric vehicles (H&EVs) dramatically influenced the automotive sector in the last years. It was predicted the EVs sales will increase to 180 million in 2045, with a total amount of circulating EVs worldwide of 530 million, outselling the conventional cars in about 20 years (Gao et al., 2018).

The main component of EVs is the battery, mainly with Lithium-Ion chemistry (LIBs), the most competitive ones in terms of costs and performances for the near and mid future (Sonoc et al., 2015).

LIBs ensure high energy density, good cycles longevity and a wide T range of use, satisfying EV requirements particularly with NMC, LFP and LMO chemistries (Winslow et al., 2018). However, once reached the 80% of residual capacity ($\approx$8–10 years), EV LIBs must be substituted in the vehicle (Natkunarajah et al., 2015; Rohr et al., 2017). Considering the increase of post-use LIBs packs from 1.4 million to 6.8 million by 2035, the introduction of a Circular Economy strategy for LIBs is strongly recommended to exploit all residual properties and to recover valuable metals from the cathode (Winslow et al., 2018; Rohr et al., 2017).

Along with the necessity to redesign and homogenize LIBs packs (Gaines, 2014), environmentally friendly alternatives must be encouraged against landfill and incineration, responsible of environmental contamination (Lv et al., 2018; Xu et al., 2008). In particular, reuse and remanufacturing allow the conservation of natural resources and a lower energy consumption, while recycling prevents safety issues, increases economic and ecological savings reducing dependence on foreign resources and satisfies always stricter regulations (Rohr et al., 2017; Gaines, 2014; Rahman, 2017; Hanisch et al., 2015).

For both routes, LIBs disassembly is a crucial step to decrease the size and pre-sort the target components (Hanisch et al., 2015; Jovane et al., 1993). It consists in the separation of connecting and structural components and it is currently performed manually due to the high variability of post-use LIB models (Wegener et al., 2015).

2. Disassembly of automotive Li-Ion batteries and scope of this work

Since the disassembly phase plays a central role in the recovery of EV batteries, this section investigates the typical structure of the product, the complexity of operative tasks and its potential hazards as fundamentals of the developed optimization model.

---

* Corresponding author.
E-mail address: luca.gentilini@polimi.it (L. Gentilini).
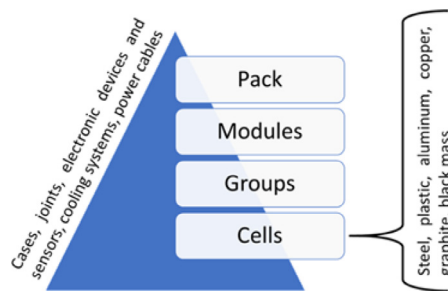
Fig 1. Hierarchical structure of a battery pack.
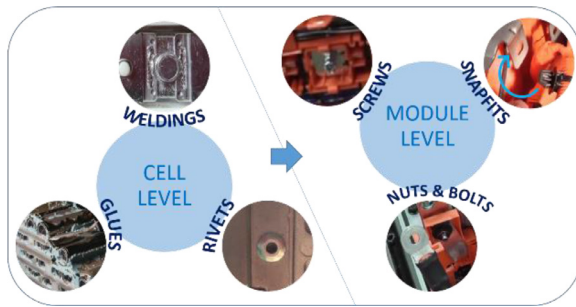
Fig. 2. Examples of joints present in automotive LIBs packs.

2.1. Modularity of e-mobility batteries

The founding elements of EV LIBs are the cells, able to convert the stored chemical energy into electrical energy through redox reactions at the interface of electrodes (Bernardes et al., 2004). Many commercial Li-Ion cells cannot provide the energy capacity to achieve the needed EVs autonomy and at the lowest hierarchical level cells are connected in parallel strings, namely *groups of cells* (see Fig. 1), to increase the capacity. Moreover, a Li-Ion cell has a fixed nominal voltage of 3.6–3.8 V and in order to reach the final voltage of the pack, generally greater than 300 V, it has to be connected in series strings. The set of single cells or groups forms *battery modules*, finite and discrete sub-components, then aggregated through series connections into the final *pack*. Complementary components as cases, electronics, cooling systems and power junctions are also available in every commercial e-mobility battery.

The type of physical and electric joints dramatically changes among modules or among cells (see Fig. 2): while to assemble different modules reversible joints (as screws or plugs) are preferred, cells and other components which sum in the single module are often assembled with non-reversible joints as welding and glue. For these reasons, it is common to consider two different disassembly phases, one from pack to modules level and one from modules to cells level.

2.2. Main phases of e-mobility batteries disassembly

Battery packs are different for every manufacturer and car model. Nevertheless, both relying on previous studies available in literature (Wegener et al., 2015, 2014; Schwarz et al., 2018) and on authors' practical experience, it is possible to find architectural similarities between different battery models which enable a generalization of the battery disassembly process (see Fig. 3):

- Covers removal. The core electric components of every battery are protected by external covers which have to be removed before anything else.
- Service plug or safety fuse removal. In each battery pack, a plug or fuse which splits in half the overall battery voltage is avail-

Fig. 3. Structure of a Nissan Leaf battery pack.

able and easily accessible under the external covers. For safety reasons, this operation should be done as soon as possible.
- Coolant removal. Some EV battery packs rely on liquid coolant to maintain the Li-Ion cells at proper operational temperature. The cooling circuit is unique for the whole battery pack. It is therefore suitable to remove the coolant liquid in the early stages of the battery pack disassembly.
- Junction block removal. The junction block, namely the set of power and low voltage electric plugs which connect the battery to the powertrain and to the car electronic units, is typically a discrete component separated from the core of the battery.
- Battery Management System (BMS) removal. Namely the set of printed circuit board, sensors and cables in charge of the battery cells monitoring and management. It can be spread at battery modules level or central and unique for the whole battery. In this case, it can be disassembled at the early stages.
- Battery modules removal. Modules are one-by-one detached to undergo dedicated downstream treatments.

2.3. Hazards in battery disassembly

Each of the macro phases above described is made of several single tasks to be accomplished, which require different tools and which do not consider a unique tasks sequence. Moreover, for the nature of the product to be disassembled, different kind of hazards have to be considered (Diekmann et al., 2018):

- Electrical risk. An EV battery pack is typically around 350 V. At this voltage, electric hazards for the operator are significant and a discharge up to a safety threshold is not recommended because it takes long times and irreversibly damages cells hindering reuse and remanufacturing. Moreover, the temperature growth due to joule effect during short circuits can be the cause of subsequent hazardous phenomena.
- Chemical hazards. Li-Ion cells contain carcinogenic materials as nickel and cobalt oxides as well as toxic gases.
- Thermal runaway. Li-Ion batteries embed highly flammable materials as the electrolyte solvents. The single cell temperature growth indirectly spread the heat to the next cells. If the heat spread is strong enough, these new cells chemically degrade and explode, starting a breakdown chain which can reach the whole battery.

For the disassembly phase, the major risk is the electrical shock because tasks are performed manually and, if the battery is intact, chemical emissions and temperature changes are not probable. Severely damaged batteries, in fact, are treated with *ad hoc* procedures and at the end of thermal runaway no residual voltage or battery functionalities are left.

2.4. Scope of the paper

Being the disassembly of automotive end-of-life LIB packs complex and hazardous, it is necessary to create decision support tools able to guide the operators through the tasks sequence with the

lower associated risk. Nevertheless, decision tools have not yet been developed and the only supports are given by governmental guidelines, standards, codes, etc. which define a threshold voltage where specific DPIs are needed (National Fire Protection Association, 2018).

This work presents a mathematical model to determine the disassembly sequence that guarantees the minimal exposure of the operator to hazardous voltages, greater than a pre-defined threshold. The model takes into account the mechanical and electrical architecture of the battery, the limit hazardous voltage as well as the tasks needed to reach the desired disassembly level. For each battery model the tool is executed once, relying on nominal voltages of the modules, then the defined optimal procedure could be replicated for all the other similar LIB packs every time needed.

Since the voltage of single battery modules (typically around 30–70 V) is below the limit hazardous voltage (National Fire Protection Association, 2018), the proposed model is built to analyze and optimize the pack-to-modules disassembly phase. In the module-to-cells phase, different risks are more relevant than the electric shock hazard (for example the risk of short-circuit within the cells), therefore different decision support tools are more suitable to analyze that phase.

3. Safety-oriented disassembly optimization model

The model works at the pack-to-modules level and takes in consideration the T tasks required to disconnect completely all the M modules of the battery pack. Furthermore, the model assumes that tasks are performed one by one (no parallelism) and that the operator is exposed to risks only when he is performing a task; therefore, no setup-times or preparation tasks are considered.

3.1. Mathematical modeling of the e-mobility battery disassembly process

Since modules are placed in series, their initial connections are conveniently represented by means of a lower-diagonal binary matrix $C = [c_{i,j}]_{M \times M}$ where each row i represents the series of connections from module 1 to module i, $1 \le i \le T$. Formally:

$$c_{i,j} = \begin{cases} 1 & if\ i \le \hat{j}\ module\ i\ is\ in\ series\ with\ j \\ 0 & otherwise \end{cases}$$

The single voltages of each module are instead collected in a vector v where each entry v_i corresponds to the residual voltage of the ith module.

According to this representation it is easy to verify that the product $C \times v^T$ provides a vector where each entry corresponds to the cumulative voltage at the ith module. For example, assuming a battery pack composed of four modules, we have:

$$C \times v^T = \begin{bmatrix} 1 & 0 & 0 & 0 \\ 1 & 1 & 0 & 0 \\ 1 & 1 & 1 & 0 \\ 1 & 1 & 1 & 1 \end{bmatrix} \times [3\quad 4.5\quad 6.\quad 2.8]^T = \begin{bmatrix} 3 \\ 7.5 \\ 13.5 \\ 16.3 \end{bmatrix} \quad (1)$$

Tasks are modeled by considering: (i) the time required to execute them; their precedencies; the possible electrical disconnections generated by the execution of the tasks. Formally, a vector $t = [t_k]_{1 \times T}$ is used to collect the average times of the tasks in such a way that entry t_k corresponds to the time required on average to execute the kth task. Task precedencies are collected into a matrix $P = [p_{k,k'}]_{T \times T}$ where entry $p_{k,k'}$ is equal to one only if task k directly depends on task k' and is equal to zero otherwise. The effects of task executions are represented by means of disconnection matrices $E_k = [e_{k,i,j}]_{M \times M}$, $1 \le k \le T$, that characterize the disconnections generated by the task. The entries of E_k are defined as

follows:

$$e_{k,i,j} = \begin{cases} 1 & if\ j < i\ and\ the\ kth\ task\ disconnects\ parts\ i\ and\ j \\ 0 & otherwise \end{cases}$$

For example, a task that disconnects the second and the third module in a battery pack composed of four modules has a disconnection matrix equal to:

$$E = \begin{bmatrix} 0 & 0 & 0 & 0 \\ 0 & 0 & 0 & 0 \\ 1 & 1 & 0 & 0 \\ 1 & 1 & 0 & 0 \end{bmatrix} \quad (2)$$

By subtracting a disconnection matrix to the connection matrix C, we are able to represent the disconnection of modules during the disassembly and the consequent generation of two independent series of modules. For example, by applying the disconnection matrix in Eq. (2) to the example in Eq. (1), we have

$$(C - E) \times v^T = \left(\begin{bmatrix} 1 & 0 & 0 & 0 \\ 1 & 1 & 0 & 0 \\ 1 & 1 & 1 & 0 \\ 1 & 1 & 1 & 1 \end{bmatrix} - \begin{bmatrix} 0 & 0 & 0 & 0 \\ 0 & 0 & 0 & 0 \\ 1 & 1 & 0 & 0 \\ 1 & 1 & 0 & 0 \end{bmatrix} \right)$$

$$\times \begin{bmatrix} 3 & 4.5 & 6. & 2.8 \end{bmatrix}^T = \begin{bmatrix} 3 \\ 7.5 \\ 6 \\ 8.8 \end{bmatrix} \quad (3)$$

which provides a vector containing the cumulative voltages of the two series generated by the electrical disconnection introduced between the second and third module.

Given the data described above, a threshold for the maximum voltage v_{max}, and a decisional matrix $X = [x_{k,s}]_{T \times T}$ where the entry $x_{k,s}$ is equal to one if and only if the kth corresponds to the sth execution, we can formalize the optimization problem as

$$\min \sum_{k=1}^{T} t_k \sum_{s=1}^{T} x_{k,s} \quad (4)$$

subject to

$$\sum_{y}^{T} x_{k,y} \le 1, \forall k \in [1, T] \quad (5)$$

$$\sum_{y}^{T} x_{y,k} \le 1, \forall k \in [1, T] \quad (6)$$

$$\sum_{z=1}^{T} \sum_{y=1}^{s-1} \left(x_{z,y} \cdot p_{k,z} \right) - x_{k,s} \sum_{z=1}^{T} p_{k,z} \ge 0, \forall k, s \in [1, T] \quad (7)$$

$$\sum_{j=1}^{M} \left(c_{i,j} - \sum_{k=1}^{T} e_{k,i,j} \sum_{z=1}^{T} x_{k,t} \right) * v_j \le v_{max}, \forall i \in [1, M] \quad (8)$$

The first constraint imposes that the execution of a task can occur at the most one time; Vice versa, the second constraint avoids that two or more tasks are performed during the same step. These two constraints are easily verified by observing that Eq. (5) imposes that each row of X sums at the most to one and equation Eq. (6) imposes the same constraint to the columns.

The third constraint instead refers the precedencies and guarantees that they are respected. In particular, the term on the l.h.s. of Eq. (7) (referred as q from now-on) checks that the precedencies of the task k have been executed during the previous $(s - 1)$ steps whereas the term on the r.h.s. (referred as b) is equal to the total number of precedencies only if the kth has been executed as sth step. Therefore, the relation $q \ge b$ always holds when task k

is not executed as sth step whereas if k is executed then the constraint is verified only if $q = b$ which corresponds to the case in which the number of dependencies required is equal to the number of dependencies executed. Note that the product between $x_{z, y}$ and $p_{k, z}$ guarantees that only the tasks corresponding to the direct precedencies are taken into account.

As last, the fourth constraint checks if the voltage of each series created by the disconnections satisfies the maximum allowed. Eq. (8) generalizes Eq. (3) by considering all the disconnections created by executing the tasks.

Note that since we consider the cumulative voltages at each module there is no need to use a *max* function to control the voltage of each series of module that is generated during the disassembly.

3.2. Search algorithm to find the optimal disassembly sequence

The search algorithm is based on a decisional tree where each node describes the status of the tasks. In particular, a task can be: (i) *blocked* (B) when its dependencies have not been executed; (ii) *ready* (R) when its dependencies have been executed but the task has not been performed; (iii) *executed* (E) when the task has been executed. The status of the task is conveniently collected in a status vector $n \in [B, R, E]^T$.

The decisional tree is built in such a way that there is only one root node representing the state in which all the tasks are blocked but those with no dependencies which are in the *ready* state; the tree has finite dimension and its maximum height is equal to the number of tasks. Node connections represent the execution of a task therefore, each node varies from its father because of a task that changed from R to E and, possibly, from tasks that have been unblocked by the execution of the task.

The tree is explored by using a breadth-first-search (BFS) with a fan-out equal to the number of ready tasks. Furthermore, by taking track of the states that have been already visited and the current optimal solution it is possible to trim the tree from those branches that corresponds to not optimal solutions or to permutations of the same solutions.

In order to provide an example, consider a battery disassembly problem with the following parameters:

$$
\mathbf{P} = \begin{bmatrix} 0 & 0 & 0 & 0 \\ 1 & 0 & 0 & 0 \\ 0 & 0 & 0 & 0 \\ 0 & 0 & 1 & 0 \end{bmatrix}, \nu = \begin{bmatrix} 0.5 \\ 2.5 \\ 0.5 \\ 2.5 \end{bmatrix}, \mathbf{t} = \begin{bmatrix} 5 \\ 3 \\ 2 \\ 5 \end{bmatrix}, \mathbf{E}_1 = \begin{bmatrix} 0 & 0 & 0 & 0 \\ 0 & 0 & 0 & 0 \\ 0 & 0 & 0 & 0 \\ 1 & 1 & 1 & 1 \end{bmatrix},
$$

$$
\mathbf{E}_2 = \begin{bmatrix} 0 & 0 & 0 & 0 \\ 1 & 0 & 0 & 0 \\ 1 & 0 & 0 & 0 \\ 0 & 0 & 0 & 0 \end{bmatrix}, \mathbf{E}_3 = \begin{bmatrix} 0 & 0 & 0 & 0 \\ 0 & 0 & 0 & 0 \\ 0 & 0 & 0 & 0 \\ 0 & 0 & 0 & 0 \end{bmatrix}, \mathbf{E}_4 = \begin{bmatrix} 0 & 0 & 0 & 0 \\ 0 & 0 & 0 & 0 \\ 1 & 1 & 0 & 0 \\ 1 & 1 & 0 & 0 \end{bmatrix} \quad (9)
$$

The precedencies are such that at the beginning only tasks 1 and 3 can be executed. Task 1 disconnects the fourth module from the others whereas task 3 does not disconnect modules. Thus, the root node has two child nodes. After the execution of task 1, it is possible to perform task 2 and after the execution of task 3 it is possible to execute task 4. Task 2 removes the connection between the first module and the second whereas task 4 remove the connection between the second and the third module. Therefore, by executing tasks 1 and 2, the total voltage of each module series satisfies the requirement as well as by performing tasks 3 and 4. However, the latter is the optimal solution because it requires a smaller execution time.

It is important to point out, how the BFS makes possible to not explore nodes that have been already encountered on other branches. In reference to Fig. 4, this is the case of node $|E, R, E, R|$ which is encountered first as child of $|E, R, R, B|$ and then as child of $|R, B, E, R|$.

Table 1
Components of the Toyota Prius battery pack, see Fig. 5.

Component	Description
1	Service plug cover
2	Cover locker
3	Front cover 1
4	Front cover 2
5	Front cover 3
6	Upper cover
7	Service plug
8	Safety fuse
9	BMS
10	Battery heater relay
11	Negative junction block
12	Positive junction block
13	Left metal frame
14	Right metal frame
15a	Module a
15b	Module b
15c	Module c
15d	Module d
15e	Module e
16	Battery pack wire (low voltage harness)
17a	Shield reinforcements a
17b	Shield reinforcements b
17c	Shield reinforcements c
17d	Shield reinforcements d
18a	Module side gas venting a
18b	Module side gas venting b
18c	Module side gas venting c
18d	Module side gas venting d
18e	Module side gas venting e
19	Battery heaters
27	Service plug circuit
32	Battery pack gas venting
33	Battery tray

4. Validation of the model, the 2017 Toyota Prius Prime use case

For the validation of the approach, the "2017 Toyota Prius Prime" battery has been chosen. Introduced on the market in 1997, the Toyota Prius has been the first mass produced and probably the most iconic hybrid electric car sold worldwide.

The battery pack has 8.79 kWh and a nominal voltage of 351.5 V, obtained by the connection of 95 prismatic cells of 3.7 V each, in a 95s1p configuration (Toyota, 2017). In particular, the pack (Fig. 5 and Table 1), contains 5 modules of 19 cells each resulting a module voltage of 70.3 V. The input data of the model are summarized in Table 2.

To provide a more robust validation of the proposed model, this result has been compared to a "time optimizing" scenario, where the disassembly tasks sequencing is defined minimizing the set-up times (not explicitly considered in the modeling phase presented in this paper), both concerning tool changes as well as operator moving and positioning. The "time optimizing" sequence has been empirically assessed by the authors, by finding the sequence of link removals which minimizes the set-up times, given by the number of tool changes and the link-link moving distance. The two disassembly strategies are compared in Table 3.

The time-minimizing disassembly tasks sequencing returns an operator hazardous voltage exposure time of 477 s, nearly the 50% more of the exposure in optimal safety-oriented disassembly sequencing conditions. Being the modules 70.3 V each, to overcome the 100 V threshold, all of the modules have to be detached. The time-minimizing strategy postpones the last electrical disconnection late in the tasks ranking, thus the disassembly is made for most of the time with electrical hazard. The safety-oriented sequencing decreases this time of the 33%, resulting in a concrete safety improvement for the operator.
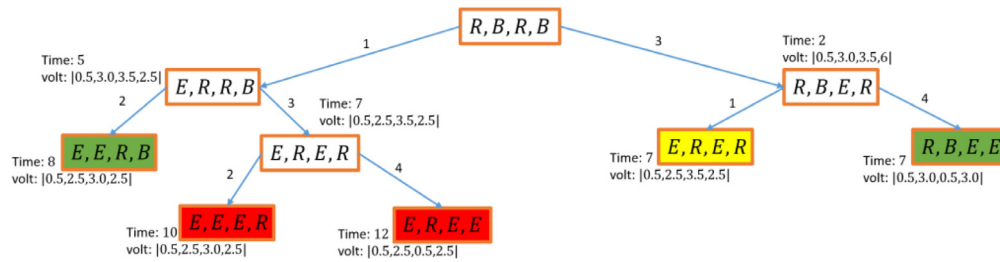
Fig. 4. Example of the decisional tree used to solve the optimization problem; green states corresponds to possible solutions; yellow states are states already visited and red states are states that do not need to be explored further.

Table 2
Decision support tool inputs summary.

t_k, time required for task k accomplishment	$\sum_{k=1}^{T} t_k$, total disassembly time	v_{max}, hazardous voltage threshold[a]	T, total number of tasks
$4\,s \leq t_k \leq 16\,s \ \forall k \in [1, T]$	532 s	100	69

[a] The hazardous voltage threshold has been set according to National Fire Protection Association (2018).

Table 3
Safety-oriented and time-oriented disassembly strategies comparison.

Disassembly strategy	Number of tasks over the voltage threshold	Disassembly time over the voltage threshold
Safety oriented	41/69	320 s/532 s
Time oriented	64/69	477 s/532 s
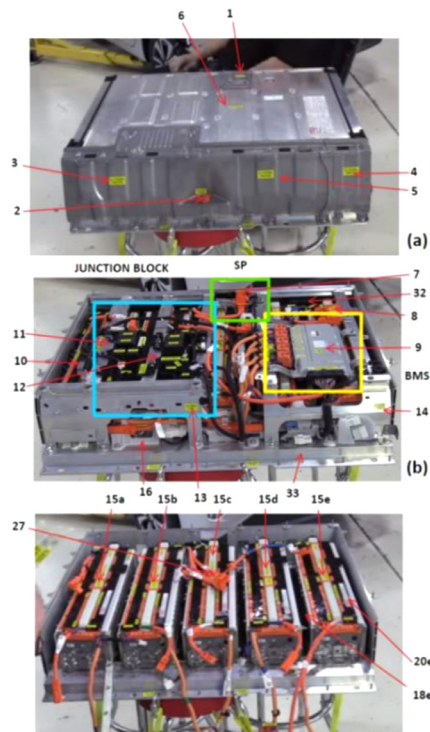
Fig. 5. The 2017 Toyota Prius Prime battery pack.

5. Conclusion and further developments

According to the need of a Circular Economy approach for end-of-life H&EV batteries, a mathematical model which minimizes the electric shock hazard of manual disassembly is presented. The aim is to guarantee both the operator safety and the preservation of battery residual functionality, identifying the optimal tasks sequence from the pack to the module level.

The model should now be applied to a wider set of commercial products to exploit its potential. Moreover, the model can be improved, for example considering not only the full disassembly of the battery, but only of target modules and sub-components. Also, the optimization algorithm developed can be exploited considering different objective functions.

Even more important, this work should not provide a stand-alone contribution to the industrial topic but should be seen as part of a wider set of studies able to create the backbone of a knowledge driven process chain for the value recovery of LIBs.

CRediT authorship contribution statement

Luca Gentilini: Conceptualization, Methodology, Validation, Investigation, Writing - original draft, Writing - review & editing, Visualization. **Elena Mossali:** Conceptualization, Investigation, Writing - original draft, Writing - review & editing, Visualization. **Alessio Angius:** Methodology, Software, Validation, Writing - original draft, Writing - review & editing, Visualization. **Marcello Colledani:** Conceptualization, Methodology, Validation, Investigation, Writing - original draft, Writing - review & editing, Visualization, Supervision.

Acknowledgments

References

Bernardes, A.M., Espinosa, D.C.R., Tenório, J.A.S., 2004. Recycling of batteries: a review of current processes and technologies. J. Power Sour. 130, 291–298. doi:10.1016/j.jpowsour.2003.12.026.

Diekmann, J., Grützke, M., Loellhoeffel, T., Petermann, M., Rothermel, S., Winter, M., Nowak, S., Kwade, A., 2018. Potential dangers during the handling of lithium-ion batteries. In: Kwade, A., Diekmann, J. (Eds.), Recycling of Lithium-Ion Batteries: The LithoRec Way. Springer International Publishing, Cham, pp. 39–51. doi:10.1007/978-3-319-70572-9_3.

Gaines, L., 2014. The future of automotive lithium-ion battery recycling: charting a sustainable course. Sustain. Mater. Technol. 1–2, 2–7. doi:10.1016/j.susmat.2014.10.001.

Gao, W., Liu, C., Cao, H., Zheng, X., Lin, X., Wang, H., Zhang, Y., Sun, Z., 2018. Comprehensive evaluation on effective leaching of critical metals from spent lithium-ion batteries. Waste Manag. 75, 477–485. doi:10.1016/j.wasman.2018.02.023.

Hanisch, C., Loellhoeffel, T., Diekmann, J., Markley, K.J., Haselrieder, W., Kwade, A., 2015. Recycling of lithium-ion batteries: a novel method to separate coating and foil of electrodes. J. Clean. Prod. 108, 301–311. doi:10.1016/j.jclepro.2015.08.026.

Jovane, F., Alting, L., Armillotta, A., Eversheim, W., Feldmann, K., Seliger, G., Roth, N., 1993. A key issue in product life cycle: disassembly. CIRP Ann. 42, 651–658. doi:10.1016/S0007-8506(07)62530-X.

Lv, W., Wang, Z., Cao, H., Sun, Y., Zhang, Y., Sun, Z., 2018. A critical review and analysis on the recycling of spent lithium-ion batteries. ACS Sustain. Chem. Eng. 6, 1504–1521. doi:10.1021/acssuschemeng.7b03811.

National Fire Protection Association, 2018. NFPA 70E® Standard for Electrical Safety in the Workplace®.

Natkunarajah, N., Scharf, M., Scharf, P., 2015. Scenarios for the return of lithium-ion batteries out of electric cars for recycling. Proc. CIRP 29, 740–745. doi:10.1016/j.procir.2015.02.170.

Rahman, A., 2017. Lithium battery recycling management and policy. IJETP 13, 1. doi:10.1504/IJETP.2017.10001405.

Rohr, S., Müller, S., Baumann, M., Kerler, M., Ebert, F., Kaden, D., Lienkamp, M., 2017. Quantifying uncertainties in reusing lithium-ion batteries from electric vehicles. Proc. Manuf. 8, 603–610. doi:10.1016/j.promfg.2017.02.077.

Schwarz, T.E., Rübenbauer, W., Rutrecht, B., Pomberger, R., 2018. Forecasting real disassembly time of industrial batteries based on virtual MTM-UAS data. Proc. CIRP 69, 927–931. doi:10.1016/j.procir.2017.11.094.

Sonoc, A., Jeswiet, J., Soo, V.K., 2015. Opportunities to improve recycling of automotive lithium ion batteries. Proc. CIRP 29, 752–757. doi:10.1016/j.procir.2015.02.039.

Toyota, OM47A88U – Toyota 2017 Prius Prime Owner's Manual, (2017). https://www.toyota.com/t3Portal/document/om-s/OM47A88U/pdf/OM47A88U.pdf (accessed September 30, 2019).

Wegener, K., Andrew, S., Raatz, A., Dröder, K., Herrmann, C., 2014. Disassembly of electric vehicle batteries using the example of the Audi Q5 hybrid system. Proc. CIRP 23, 155–160. doi:10.1016/j.procir.2014.10.098.

Wegener, K., Chen, W.H., Dietrich, F., Dröder, K., Kara, S., 2015. Robot assisted disassembly for the recycling of electric vehicle batteries. Proc. CIRP 29, 716–721. doi:10.1016/j.procir.2015.02.051.

Winslow, K.M., Laux, S.J., Townsend, T.G., 2018. A review on the growing concern and potential management strategies of waste lithium-ion batteries, Resources. Conserv. Recycl. 129, 263–277. doi:10.1016/j.resconrec.2017.11.001.

Xu, J., Thomas, H.R., Francis, R.W., Lum, K.R., Wang, J., Liang, B., 2008. A review of processes and technologies for the recycling of lithium-ion secondary batteries. J. Power Sour. 177, 512–527. doi:10.1016/j.jpowsour.2007.11.074.